Leakage mechanisms in $BiFeO_3$ thin films

Gary W. Pabst, Lane W. Martin,[a] Ying-Hao Chu, and R. Ramesh
Department of Materials Science and Engineering, University of California, Berkeley, Berkeley, California 94720 and Lawrence Berkeley National Laboratory, Berkeley, California 94720

(Received 18 December 2006; accepted 13 January 2007; published online 13 February 2007)

The authors report results of transport studies on high quality, fully epitaxial $BiFeO_3$ thin films grown via pulsed laser deposition on $SrRuO_3/DyScO_3$ (110) substrates. Ferroelectric tests were conducted using symmetric and asymmetric device structures with either $SrRuO_3$ or Pt top electrodes and $SrRuO_3$ bottom electrodes. Comparison between these structures demonstrates the influence of electrode selection on the dominant transport mechanism. Analysis of film electrical response suggests Poole-Frenkel emission as the limiting leakage current mechanism in the symmetric structure. Temperature dependent measurements yield trap ionization energies of ~0.65–0.8 eV. No clear dominant leakage mechanism was observed for the asymmetric structure. © *2007 American Institute of Physics*. [DOI: 10.1063/1.2535663]

With an ever-expanding demand for data storage, transducers, and microelectromechanical systems applications, materials with superior ferroelectric and piezoelectric responses are of great interest. The $Pb(Zr,Tr)O_3$ (PZT) family of materials has served as the cornerstone of these devices to date. A critical drawback of this material, however, is its toxicity due to the lead content. Recently, lead-free ferroelectric $BiFeO_3$ (BFO) has attracted a great deal of attention because of its superior properties in both epitaxial and polycrystalline thin films.[1–4] Its remnant polarization P_r and out-of-plane converse piezoelectric coefficient d_{33} are comparable to those of the tetragonal, Ti-rich PZT system. Moreover, due to a high Curie temperature (T_C=820–850 °C),[5,6] it also shows great promise for use in high temperature applications. Additionally, previous studies have successfully integrated BFO films on Si substrates by using a $SrTiO_3$ (STO) template layer and $SrRuO_3$ (SRO) bottom electrode.[7,8] These films exhibited large coercive fields and a large leakage current, which might limit the applicability of BFO in devices. Such drawbacks have prompted a number of studies attempting to reduce the leakage in BFO through the use of chemical dopants.[9–12] In fact, Fujitsu Microelectronics America, Inc. recently announced the production of 65 nm ferroelectric random access memory devices using Mn-doped BFO to reduce the leakage current.[13] In this letter we focus our attention on the mechanisms that lead to the large leakage current in high quality BFO thin films. This will, in turn, help guide future work to integrate BFO into functional microelectronic devices.

Thin film heterostructures of BFO (~175 nm) and SRO (~50 nm) were grown on $DyScO_3$ (DSO) (110) single crystal substrates via pulsed laser deposition at 700 °C and 100 mTorr partial pressure of oxygen. X-ray diffraction (Panalytical X'Pert MRD Pro) shows that BFO films grown on DSO substrates are single phase and exhibit very narrow rocking curves for the 002-pseudocubic diffraction peak of BFO (full width at half maximum) of 0.055° pointing to the extremely high quality and epitaxial nature of these films. Additionally, at these thicknesses, the BFO films appear to relax to a derivative of the bulk rhombohedral structure[14] as confirmed by a φ scan of the rhombohedrally nondegenerate 210_R reflection in BFO.[15,16] Note that we do not rule out an additional slight monoclinic distortion to the lattice. Through careful control of the growth of the underlying SRO bottom electrode layer, we can engineer the structural domain configuration of the SRO and thereby affect control over the BFO domain structure.[17] The samples measured here exhibit multivariant domain structures in the BFO films as imaged via piezoforce microscopy (not shown here). Top SRO electrodes (32 μm diameter) were deposited *ex situ* at room temperature and then annealed in oxygen at 600 °C for 30 min to facilitate crystallization. Finally, approximately 150 nm of platinum was sputtered onto the SRO top electrodes to facilitate a low resistance contact. Ferroelectric and leakage measurements were carried out using a Radiant Technologies Inc. RT6000S ferroelectric test system.

The ferroelectric nature of these films is demonstrated in Figs. 1(a)–1(d). The polarization–electric field (P-E) hysteresis loops are sharp and square and yield a $2P_r$ value of 120–130 $\mu C/cm^2$. Such values are consistent with previ-

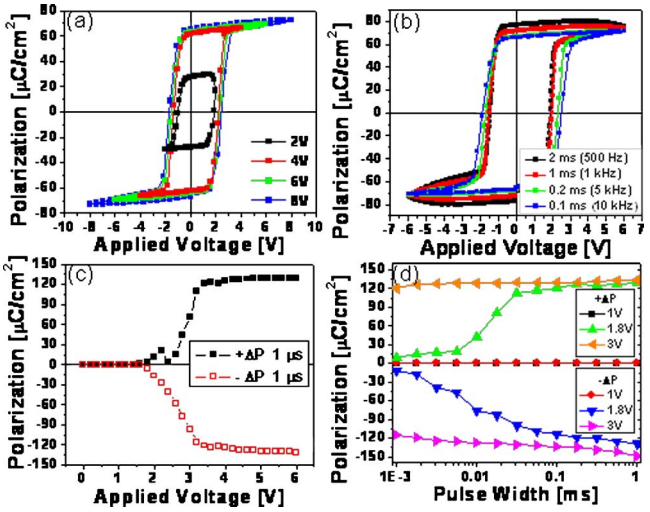

FIG. 1. (Color online) Ferroelectric data demonstrating intrinsic ferroelectricity and sharp hysteresis. Included are (a) a voltage series, (b) a frequency series of P-V loops, and PUND measurements for (c) varying voltage at 1 μs and (d) varying pulse width for given voltages.

[a]Author to whom correspondence should be addressed; electronic mail: lwmartin@berkeley.edu

ously measured values for BFO grown on STO and STO/Si substrates.[1,7,8,15] The saturation of the hysteresis loops as a function of voltage [Fig. 1(a)] is key evidence of intrinsic ferroelectricity in the films. The weak frequency dependence of the loops [Fig. 1(b)] also supports this claim. To more closely investigate the ferroelectric properties, pulsed polarization positive up negative down (PUND) measurements were made with a varying field at a pulse width of 1 μs [Fig. 1(c)] and with a varying pulse width at fixed voltages [Fig. 1(d)]. The switched polarization values (ΔP) of these measurements match well with the $2P_r$ values obtained from the *P-E* loops. Note also the weak pulse width dependence of Fig. 1(d) once saturation is reached, yet another indication of robust intrinsic ferroelectricity.

The literature on possible leakage current limiting mechanisms for BFO and other similar ferroelectric perovskite oxides discusses a large number of possible mechanisms. These mechanisms fall into two categories, bulk-limited and interface-limited conduction. Of all the possible mechanisms, we consider three in this letter that are commonly observed in other perovskite oxides. The first mechanism is interface-limited Schottky emission, which arises from a difference in Fermi levels between a metal (electrode) and an insulator or semiconductor (film). The energy difference creates a potential barrier between the metal and insulator that charges must overcome. The current density across a Schottky barrier is[18]

$$J_S = AT^2 \exp - \left[\frac{\Phi}{k_B T} - \frac{1}{k_B T} \left(\frac{q^3 V}{4\pi\varepsilon_o K d} \right)^{1/2} \right], \quad (1)$$

where A is the Richardson constant, Φ is the height of the Schottky barrier, K is the dielectric constant of the film, and d is the sample thickness. The second mechanism considered is bulk-limited space-charge-limited conduction (SCLC). The limitation arises from a current impeding space charge forming as charges are injected into the film from the electrode at a rate faster than they can travel through the film. The current density for SCLC is[19,20]

$$J_{\mathrm{SCLC}} = \frac{9\mu\varepsilon_o K}{8} \frac{V^2}{d^3}, \quad (2)$$

where μ is carrier mobility. The third mechanism is bulk-limited Poole-Frenkel emission. This conduction mechanism involves the consecutive hopping of charges between defect trap centers. The ionization of the trap charges can be both thermally and field activated. The conductivity for Poole-Frenkel emission is[21]

$$\sigma_{\mathrm{PF}} = c \exp - \left[\frac{E_I}{k_B T} - \frac{1}{k_B T} \left(\frac{q^3 V}{\pi\varepsilon_o K d} \right)^{1/2} \right], \quad (3)$$

where c is a constant and E_I is the trap ionization energy.

Typical leakage data (*I-V*) as a function of applied voltage for a 175 nm thick film are shown in Fig. 2(a). Data for both positive and negative biases have been graphed on the same axis. By plotting our data in various manners as a function of voltage, we can quickly gain insight into the nature of the leakage mechanism. According to Eq. (2) above, SCLC can be investigated by plotting the leakage data as J vs V^2, as shown in Fig. 2(b). If SCLC were the dominant leakage mechanism, a straight fit to the data in Fig. 2(b) would be possible. Since it shows an exponential trend, SCLC can be ruled out as the leakage current limiting mechanism for these BFO thin films for the voltage range measured.

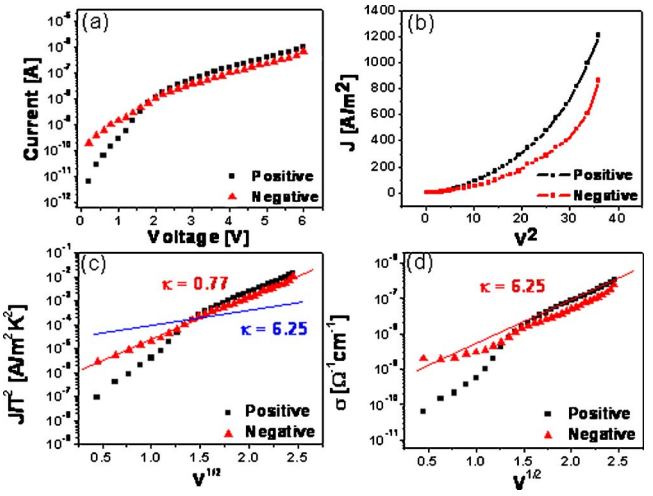

FIG. 2. (Color online) Typical *I-V* characteristics of the Pt/SRO/BFO/SRO/DSO thin film structures. (a) Typical leakage data. Various fits of these data are shown to help determine the leakage mechanism: (b) SCLC, (c) Schottky barrier, or (d) Poole-Frenkel emission.

Similar analysis of Eqs. (1) and (3) tells us that if a Schottky barrier controls the leakage current or if Poole-Frenkel emissions are dominant, semilog plots of J/T^2 vs $V^{1/2}$ and σ vs $V^{1/2}$, respectively, will show straight line fits to the data. Both these plots, however, will often show regions with straight fits to the data, as shown in Figs. 2(c) and 2(d). To identify which mechanism might be dominating the leakage current, it is necessary to extract the dielectric constant from the slopes of these plots. Iakovlev *et al.* report the index of refraction for BFO to be $n=2.5$;[22] thus we should expect a dielectric constant of $K=n^2=6.25$.

From the Schottky plot [Fig. 2(c)], a dielectric constant of ~0.77 is obtained for a negative bias as well as for fields above ~2 V for a positive bias. The Poole-Frenkel plot [Fig. 2(d)] on the other hand yields a dielectric constant of ~6.25 for a negative bias and a positive bias above ~2 V. Since this is the expected value of the dielectric constant and the value obtained from the Schottky plot is off by an order of magnitude, it is indicative of the leakage mechanism in these BFO films being dominated by Poole-Frenkel emissions. This is not unexpected as Poole-Frenkel emission has been identified as the dominant leakage mechanism in other ferroelectric perovskites such as PZT.[23,24] In the case of BFO, the likely trap center is the Fe ions. It is widely accepted that oxygen vacancies formed during growth cause a portion of the Fe^{3+} ions to become Fe^{2+}. These Fe ions are often considered to be responsible for the high leakage of BFO.

To determine the value of the Poole-Frenkel trap ionization energy we measured leakage as a function of temperature. Plots of σ vs $1000/T$ for fixed voltages are shown in Fig. 3(a). From these slopes, ionization energies are extracted and used to extrapolate the zero-field ionization energy [Fig. 3(b)]. The low voltages not conforming to the trend are not unexpected as we do not observe Poole-Frenkel dominating in positive bias at low fields. Fitting with the higher field data points yields a trap ionization energy of ~0.8 eV. It should be noted, however, that multiple mea-

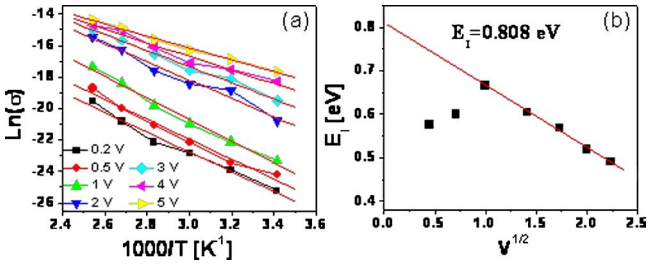

FIG. 3. (Color online) (a) Temperature dependence of conductivity with linear fits (red lines) used to extract trap ionization energies. (b) Plot of trap ionization energies from (a) in order to extrapolate the zero-field trap ionization energy.

surements yielded a range of about 0.65–0.8 eV for the trap ionization energy.

In contrast, analysis of data taken with Pt top electrodes (Pt/BFO/SRO//DSO) yielded inclusive results. Figure 4 shows data for Pt analogous to that of Fig. 2 for the Pt/SRO top electrodes. First, notice that there is a considerable asymmetry between *I-V* behavior for positive and negative biases [Fig. 4(a)], consistent with the fact that the top (Pt) and bottom (SRO) electrodes have different work functions and electron affinities. Both polarities were prepoled and the response was repeatable. At this time the origin of this behavior is unknown. The SCLC, Schottky, and Poole-Frenkel plots all show regions with reasonable fits [Figs. 4(b) and 4(c)]. The SCLC plot shows a linear fit above ~2.5 V for increasing negative bias [Fig. 4(b)]. This same region, however, also shows a near perfect match for Schottky emission [Fig. 4(c)]. The higher voltage regions of both positive and the decreasing negative biases show linear fits for the Poole-Frenkel mechanism as well [Fig. 4(c)]. The best Poole-Frenkel fit yields a dielectric constant of 5.5, which is slightly lower than the expected 6.25 but not unreasonable.

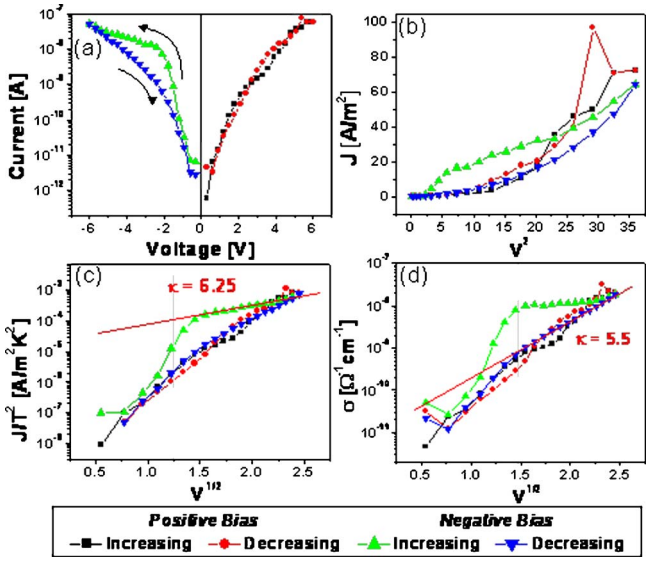

FIG. 4. (Color online) Typical *I-V* characteristics of the Pt/BFO/SRO/DSO thin film structures. (a) Typical leakage data. Various manipulations of these data are shown to help determine the leakage mechanism: (b) SCLC, (c) Schottky barrier, or (d) Poole-Frenkel emission.

These data indicate that using Pt alone as a top electrode to contact BFO films creates a capacitor with competing leakage mechanisms.

In summary, we have shown the leakage mechanism of BFO with symmetric SRO electrodes on DSO substrates to be dominated by Poole-Frenkel emission. A measured trap ionization energy of 0.65–0.8 eV may correspond to the ionization of Fe^{2+} ions. We have also shown that there is no clear dominant mechanism when Pt is used as the top electrode. Careful studies and attention must be given to choose a contact with the appropriate material properties to alleviate this effect.

This work is supported by the Director, Office of Basic Energy Sciences, Materials Sciences Division of the U.S. Department of Energy under Contract No. DE-AC02-05CH11231 and ONR-MURI Grant No. E21-6RU-G4.

[1] J. Wang, J. B. Neaton, H. Zheng, V. Nagarajan, S. B. Ogale, B. Liu, D. Viehland, V. Vaithyanathan, D. G. Schlom, U. V. Waghmare, N. A. Spaldin, K. M. Rabe, M. Wuttig, and R. Ramesh, Science **299**, 1719 (2003).
[2] W. Eerenstein, F. D. Morrison, J. Dho, M. G. Blamire, J. F. Scott, and N. D. Mathur, Science **307**, 1203 (2005).
[3] J. Wang, A. Scholl, H. Zheng, S. B. Ogale, D. Viehland, D. G. Schlom, N. A. Spaldin, K. M. Rabe, M. Wuttig, L. Mohaddes, J. Neaton, U. Waghmare, T. Zhao, and R. Ramesh, Science **307**, 5713 (2005).
[4] K. Y. Yun, M. Noda, and M. Okuyama, Appl. Phys. Lett. **83**, 3981 (2003).
[5] Y. N. Venevtsev, G. Zhadanov, and S. Solov'ev, Sov. Phys. Crystallogr. **4**, 538 (1960).
[6] G. Smolenskii, V. Isupov, A. Agranovskaya, and N. Kranik, Sov. Phys. Solid State **2**, 2651 (1961).
[7] J. Wang, H. Zheng, Z. Ma, S. Prasertchoung, M. Wuttig, R. Droopad, J. Yu, K. Eisenbeiser, and R. Ramesh, Appl. Phys. Lett. **85**, 2574 (2004).
[8] S. Y. Yang, F. Zavaliche, L. Mohaddes-Ardabili, V. Vaithyanathan, D. G. Schlom, Y. J. Lee, Y. H. Chu, M. P. Cruz, Q. Zhan, T. Zhao, and R. Ramesh, Appl. Phys. Lett. **87**, 102903 (2005).
[9] C. Wang, M. Takahashi, H. Fujino, X. Zhao, E. Kume, T. Horiuchi, and S. Sakai, J. Appl. Phys. **99**, 054104 (2006).
[10] C.-F. Chung, J.-P. Lin, and J.-M. Wu, Appl. Phys. Lett. **88**, 242909 (2006).
[11] G. L. Yuan and S. W. Or, Appl. Phys. Lett. **88**, 062905 (2006).
[12] X. Qi, J. Dho, R. Tomov, M. G. Blamire, and J. L. MacManus-Driscoll, Appl. Phys. Lett. **86**, 062903 (2005).
[13] Fujitsu Microelectronics America, Inc., Sunnyvale, CA, Press Release, 2 August 2006 (http://www.fujitsu.com/ca/en/news/pr/fma_20060802.html).
[14] F. Kubel and H. Schmid, Acta Crystallogr., Sect. B: Struct. Sci. **46**, 698 (1990).
[15] R. R. Das, D. H. Kim, S. H. Baek, C. B. Eom, F. Zavaliche, S. Y. Yang, R. Ramesh, Y. B. Chen, X. Q. Pan, X. Ke, M. S. Rzchowski, and S. K. Streiffer, Appl. Phys. Lett. **88**, 242904 (2006).
[16] G. Xu, H. Hiraka, G. Shirane, J. Li, J. Wang, and D. Viehland, Appl. Phys. Lett. **86**, 182905 (2005).
[17] Y.-H. Chu, Q. Zhan, L. W. Martin, M. P. Cruz, P.-L. Yang, G. W. Pabst, F. Zavaliche, S.-Y. Yang, J.-X. Zhang, L.-Q. Chen, D. G. Schlom, I.-N. Lin, T.-B. Wu, and R. Ramesh, Adv. Mater. (Weinheim, Ger.) **18**, 2307 (2006).
[18] W. Schottky, Naturwiss. **26**, 843 (1938).
[19] N. F. Mott and R. W. Gurney, *Electronic Processes in Ionic Crystals* (Clarendon, Oxford, 1940).
[20] M. A. Lampert and P. Mark, *Current Injection in Solids* (Academic, New York, 1970).
[21] J. Frenkel, Tech. Phys. USSR **5**, 685 (1938).
[22] S. Iakovlev, C.-H. Solterbeck, M. Kuhnke, and M. Es-Souni, J. Appl. Phys. **97**, 094901 (2005).
[23] B. Nagaraj, S. Aggarwal, T. K. Song, T. Sawhney, and R. Ramesh, Phys. Rev. B **59**, 16022 (1999).
[24] P. Zubko, D. J. Jung, and J. F. Scott, J. Appl. Phys. **100**, 114113 (2006).